12th International Symposium on Turbulence and Shear Flow Phenomena (TSFP12)
Osaka, Japan, July 19–22, 2022

INTERACTION BETWEEN WAVEPACKETS AND STREAKS IN TURBULENT JETS

Petrônio A. S. Nogueira
Aerospace Engineering
Monash University
3800, Clayton, Australia
petronio.nogueira@monash.edu

André V. G. Cavalieri
Engenharia Aeronáutica
Instituto Tecnológico de Aeronáutica
12228-900, São José
dos Campos, Brazil
andre@ita.br

Vincent Jaunet
Fluides, Thermique, Combustion
Institut PPrime
86962, Poitiers, France
vincent.jaunet@ensma.fr

Oliver Schmidt
Mechanical and Aerospace Engineering
University of California
CA 92093, La Jolla, USA
oschmidt@ucsd.edu

Peter Jordan
Fluides, Thermique, Combustion
Institut PPrime
86962, Poitiers, France
peter.jordan@univ-poitiers.fr

Daniel Edgington-Mitchell
Aerospace Engineering
Monash University
3800, Clayton, Australia
daniel.mitchell@monash.edu

ABSTRACT

We propose a formulation to study the effect of streaks in the spatial development of wavepackets. To this end, a modified version of the parabolised stability equations (PSE) linearized around a streak-containing mean flow is used, which considers a series of azimuthal wavenumbers in the solution. In the present case, streaks are obtained from experiments using spectral proper orthogonal decomposition applied to particle image velocimetry data, and extrapolated in the radial direction using a Gaussian fit. Streaks and rolls predicted by resolvent analysis are also used in the analysis to evaluate the effect of streamwise vortices in the development of the noise-generating structures. Results show that streaks non-trivially modify the spatial support of the Kelvin-Helmholtz wavepackets and their phase velocity, which may lead to changes in the sound generation efficiency of the jet. New structures across the shear layer induced by the presence of streaks are also observed further downstream for high streak amplitudes.

Introduction

Recent works have identified the presence of three structures in turbulent jets: Kelvin-Helmholtz (KH) wavepackets (Cavalieri *et al.*, 2013), Orr structures (Tissot *et al.*, 2017) and streaks (Nogueira *et al.*, 2019*a*). As summarised by Pickering *et al.* (2020), these structures are a result of distinct flow mechanisms and are dominant in different regions of the frequency-azimuthal wavenumber spectrum. The Kelvin-Helmholtz mode is generated by a linear stability mechanism caused by the presence of an inflection point in the jet base flow. These structures usually follow a spatial pattern of growth-saturation-decay, and are present at mid-high frequencies and most azimuthal wavenumbers. These structures are also responsible for most of the sound radiated at low polar angles in subsonic jets (Cavalieri *et al.*, 2012). Streaks, on the other hand, are a result of the lift-up effect (Ellingsen & Palm, 1975) and are only active at very low frequencies (Strouhal number $St_m \to 0$) and non-zero azimuthal wavenumber. Despite their high amplitude, these structures generate no sound, as they are virtually invariant in the streamwise direction. However, streaks may impact sound radiation indirectly by means of their effect on the development of the KH wavepacket, i.e., via non-linear interactions between these two structures. A study of such interaction in a reduced-order model was performed by Nogueira & Cavalieri (2021), who used a confined shear-layer model to evaluate the temporal dynamics involving streaks and wavepackets. They showed that these structures interact via oblique waves, and that streamwise elongated rolls are also an important part of the dynamics. But these results are yet to be extended for real turbulent jets.

This work aims to overcome this limitation. To achieve this, we propose a model to evaluate the interaction between these structures using PSE linearised around a streak-containing mean flow, similar to the formulation proposed by Sinha *et al.* (2016). The model allows us to track the spatial evolution of the originally axisymmetric wavepacket in the presence of streaks and to evaluate how this interaction may change its noise-producing characteristics. The paper is organised as follows: first, a formulation for the Parabolised Stability Equations for jets with streaks is presented. This is followed by a description of the methods for obtaining streaks, which are based on experimental results and resolvent analysis. Finally, a parametric sweep of streak amplitude and azimuthal wavenumber is performed, where some trends relevant for sound generation are highlighted. The paper is closed with a summary of the main conclusions.

Parabolized Stability Equations

This study is based on the parabolised stability equations (PSE) (Herbert, 1997; Gudmundsson & Colonius, 2011). The formulation considers solutions in the frequency domain ω as

$$\mathbf{q}(x,r,\theta,\omega) = \hat{\mathbf{q}}(x,r,\theta,\omega)\mathrm{e}^{\mathrm{i}\int^x \alpha(x_1)dx_1} \tag{1}$$

where both $\hat{\mathbf{q}}$ and α are slowly varying functions in the streamwise direction x, and $\mathbf{q}$ contains all flow quantities (specific volume, pressure and the three velocity components). Instead of assuming normal modes in θ, as is often the case in round jets, we consider a base flow decomposed in a series of modes in azimuth; thus, the streamwise velocity component of the base flow (and equivalently for all other components) can be written as

$$\mathbf{U}(x,r,\theta) = \mathbf{U_0}(x,r) + \frac{A_s}{2}\left[\mathbf{U_{m_s}}(x,r)\mathrm{e}^{\mathrm{i}m_s\theta} + \mathbf{U_{-m_s}}(x,r)\mathrm{e}^{-\mathrm{i}m_s\theta}\right] \tag{2}$$

where m_s is the streak azimuthal wavenumber, $\mathbf{U_{m_s}}(x,r)$ defines the shape of the streak in space, and A_s is its amplitude. This amplitude represents the maximum of the streak in (x,r) as a percentage of the maximum jet Mach number. The proposed base flow includes the zeroth component (which is simply the azimuthally and temporally averaged mean flow from experiments) and the zero-frequency component of the flow at different azimuthal wavenumbers, which can be viewed as its streaky component (Nogueira *et al.*, 2019*a*). This base flow will be used to study the effect of streaks and rolls in the development of the KH wavepacket. Using this base flow shape, the flow disturbances can be written as a sum of several azimuthal wavenumbers (Sinha *et al.*, 2016) as

$$\hat{\mathbf{q}}(x,r,\theta,\omega) = \sum_{n=-N_s}^{N_s} \mathbf{q_n}(x,r,\omega)\mathrm{e}^{\mathrm{i}(m+nm_s)\theta} \tag{3}$$

where m is the central wavenumber of the disturbances. For an originally axisymmetric wavepacket, this shape of solution becomes a sum of the $m=0$ mode and the respective streak modulation components nm_s, which are truncated to a number of harmonics N_s. Inserting equations 1, 2 and 3 into the linearized Navier-Stokes equations (NS), and gathering all terms of different powers of $m+nm_s$, we can write the equations in operator form as

$$-\mathrm{i}\omega\tilde{\mathbf{q}} + \mathbf{L_t}\tilde{\mathbf{q}} + \mathbf{B_t}\frac{\partial\tilde{\mathbf{q}}}{\partial x} + \mathrm{i}\alpha\mathbf{B_t}\tilde{\mathbf{q}} + \mathrm{i}m\mathbf{C_t}\tilde{\mathbf{q}} - m^2\mathbf{D_t}\tilde{\mathbf{q}} = 0 \tag{4}$$

where the vector $\tilde{\mathbf{q}} = [\hat{\mathbf{q}}_{-\mathbf{N}} \ldots \hat{\mathbf{q}}_{\mathbf{0}} \ldots \hat{\mathbf{q}}_{\mathbf{N}}]^T$ comprises all the modulation components. Following the PSE method, the second streamwise derivatives are neglected in the equations, and the solution is marched from a position close to the nozzle until the desired station downstream by discretizing the first streamwise derivatives using first-order implicit Euler differences. The streamwise wavenumber is updated at each step using the normalisation condition outlined in Herbert (1994), which minimizes the streamwise variation of the shape function. This formulation is similar to that developed by Sinha *et al.* (2016), with the difference that only a single azimuthal mode (and its complex conjugate) is considered in the mean flow. This considerably simplifies the analysis and also allows us to evaluate the effect of isolated streaks in wavepackets.

Streaks in turbulent jets

The present formulation requires a mean flow and the shapes of the streaks for each azimuthal wavenumber to be studied. Both resolvent analysis (Pickering *et al.*, 2020) and spectral proper orthogonal decomposition (SPOD) (Nogueira *et al.*, 2019*a*) may be used to obtain these structures in turbulent jets. Both approaches are used here. SPOD modes were obtained at vanishing frequency $St_m \to 0$ from the streamwise velocity PIV data presented in Nogueira *et al.* (2019*a*) for a Mach $M=0.4$ jet. Since these energetic structures were obtained in a limited domain, they have been extrapolated in the radial direction by means of fitting their radial structure with a Gaussian function at each streamwise step, which led to a good representation of the original data. Sample SPOD modes for $m_s = 2$, 4 and 6 are shown in figure 1. As also shown in Nogueira *et al.* (2019*a*), streaky structures decrease in length in the streamwise direction as m_s is increased, a consequence of their self-similar behaviour. For that reason, their peak also approaches the nozzle for higher m_s; in these cases, as most of the streak is located where the shear layer is thinner, they will potentially have a stronger effect on the growth of the KH.

Resolvent analysis is based on an expansion of the NS equations around a given base flow, which may be written in an input-output form as

$$-\mathrm{i}\omega\mathbf{q}' = \mathbf{L}\mathbf{q}' + \mathbf{f}' \tag{5}$$

where all variables $\mathbf{q}'(x,r,m_s,\omega)$ are considered in the frequency-azimuthal wavenumber domain, and the term $\mathbf{f}'$ gathers all non-linear terms of the equations. Rearranging the terms of equation 5, one can write

$$\mathbf{q}' = (-\mathrm{i}\omega\mathbf{I} - \mathbf{L})^{-1}\mathbf{f}' = \mathbf{R}\mathbf{f}' \tag{6}$$

A singular value decomposition of the resolvent operator $\mathbf{R}$ leads to optimal forcing and response modes of the flow for a given frequency and azimuthal wavenumber, which are directly comparable to SPOD modes if the statistics of the forcing are white in space (Towne *et al.*, 2018). Here, resolvent modes were computed for $St=0$ and $m_s=6$ as in Nogueira *et al.* (2019*b*) using the same mean flow and reduced domain. The mode shapes obtained from this method are given in figure 2, where the absolute value of all three velocity components are shown. The resulting structure looks like streaks (in the streamwise velocity component) and streamwise vortices (or rolls, in the radial and azimuthal velocity components), in agreement with the lift-up effect (not shown here because of space limitations). Comparing figures 1(c) and 2(a), it is clear that resolvent modes are more extended in the streamwise direction, not reaching a peak within the domain studied here. This is due to the fact that no eddy-viscosity model (or colored forcing) was included in these computations, which leads to a stronger misalignment between resolvent and SPOD modes (Pickering *et al.*, 2020, 2021). The differences in shapes of the streaks may also change the overall characteristics of the mean flow given in equation 2, leading to a locally thinner shear layer for the resolvent-streaks. These differences may have an effect on the development of the KH mode.

With the shapes of the streaks defined by these methods, their amplitudes A_s will be treated as a free parameter in this work. Modes resulting from resolvent analysis have fixed relative amplitudes between streaks and rolls, which removes the dependence on the rolls amplitudes in the present analysis. Further details about the experiments and simulations can be found in Nogueira *et al.* (2019*a*,*b*); Schmidt *et al.* (2018).

Results

PSE results of streak-modulated KH modes were generated for $N_s = 3$, Reynolds number $Re = 30000$, and $St = 0.4$; analysis of other frequencies led to similar results. We start with a study of the modulation induced by streaks obtained from SPOD. As mentioned earlier, SPOD was applied to the streamwise velocity component, an thus the influence of the radial and azimuthal velocities (or the rolls) was neglected. Due to the absence of data at the nozzle plane, the amplitude of the streaks at that position was also assumed to be negligible, so all modes start as axisymmetric in the spatial march.

Figure 3 shows the shapes of streak-modulated KH modes for $A_s = 6\%$ and $m_s = 2$,4 and 6, which illustrates the overall effect of the streaks in the wavepacket shapes. The most clear feature of these wavepackets is that, despite being initially axisymmetric, they have strong azimuthal non-uniformities associated with the streak azimuthal wavenumber. These structures represent axisymmetric wavepackets that grow together with oblique waves, as in Nogueira & Cavalieri (2021). For $m = 2$, the base flow that results from the superposition of streaks and the axisymmetric mean flow has an almost elliptical shape; for this case, the resulting wavepacket grows more strongly in the direction perpendicular to the major axis of the ellipse, similar to what is observed in elliptical jets (Edgington-Mitchell *et al.*, 2015). For the other azimuthal wavenumbers ($m_s = 4$ and 6), chevron-like structures are observed to grow close to the jet shear layer, which are followed by the appearance of tilted structures further downstream. Qualitatively, these structures are similar to the mushroom-like structures observed in previous locally parallel models (Lajús *et al.*, 2019; Wang *et al.*, 2021) and experiments/simulations (Alkislar *et al.*, 2007; Violato & Scarano, 2011).

Here, we are interested in the changes induced by the presence of steady streaks in the development of the KH; more specifically, changes in the growth and phase velocity of the KH are of particular interest, as these are expected to impact the acoustic far-field. In order to evaluate how the streaks affect the growth of the wavepackets, an attenuation parameter is defined as

$$\xi(x) = \left| \frac{u_{A_s}(x, r = 0)}{u_{A_s=0}(x, r = 0)} \right| \tag{7}$$

which defines the amplitude ratio between the axisymmetric wavepacket and the streak-modulated ones at the centerline.

Figure 4 shows the attenuation induced by SPOD-streaks for increasing A_s and $m_s = 2$, 4 and 6. Since all SPOD-streaks start with zero amplitude, the value of ξ is close to unity for the first few diameters, indicating that these structures possibly have too low amplitude to affect the KH mode in that region. As the streaks grow spatially, they start to have a stabilising effect on the KH. This effect increases monotonically with A_s for all values of m_s. It can also be observed that the start of the stabilisation region is usually associated with the region in space where the streaks have higher amplitudes; thus, an increase in m_s could lead to an earlier stabilisation of the KH mode, which is in line with the locally-parallel results of Lajús *et al.* (2019). In fact, the present results suggest that higher m_s streaks may be more efficient in stabilising the KH mode, as a greater reduction of ξ is obtained for high streak azimuthal wavenumber, keeping A_s constant.

The influence of the streaks in the phase velocity of the KH (defined as $c_{ph} = \omega/\alpha(x)$, with $\alpha(x)$ obtained directly from the PSE) is shown in figure 5. In contrast with the stabilisation effect seen in figure 4, this quantity is not strongly affected by the presence of streaks in the analysis. Small changes in phase velocity are observed further downstream, with increasing reduction of c_{ph} with increasing A_s and m_s. Together, results from figures 4 and 5 suggest that streaks with moderate-high amplitude and azimuthal wavenumber (within the range studied herein) may be acoustically beneficial, reducing the amplitude of the noise-generating structures and possibly making them less acoustically efficient (Jordan & Colonius, 2013; Cavalieri *et al.*, 2019).

The same quantities were computed for resolvent-streaks, which are shown in figure 6. If the rolls are neglected (figures 6(a,c)), results for moderate streak amplitude are qualitatively similar to the ones from SPOD-streaks, with a stabilisation region observed further downstream, which is also associated with a reduction of the phase velocity of the KH mode. However, these trends are strongly amplified in this case, with substantially higher reductions in both ξ and c_{ph}. A small region of destabilisation is also observed around $1.5 < x/D < 4$, which may be associated with the fact that streaks start with non-zero amplitudes in this case. Also, as shown in figure 7, the radial support of resolvent-streaks differs from SPOD-streaks, with structures more concentrated across the shear layer. These differences in spatial support leads to changes in the mean flow that could be the source of the disparity between figures 4, 5 and 6. This is exemplified in figure 7: while SPOD-streaks induce smoother radial variation in the mean flow, resolvent-streaks create stronger gradients across the shear layer, which will have an effect on the stability of the flow.

The inclusion of rolls is evaluated in figures 6(b,d). Overall, the rolls seem to intensify the effect of the streaks on the attenuation for all x/D: very close to the nozzle, a slight stabilising effect is observed with increasing A_s, followed by a strong destabilisation close to the end of the potential core. Similar to the previous cases, streaks stabilise the KH mode and reduce its phase velocity further downstream if they have moderate amplitude. However, an increase in phase velocity close to the nozzle is observed for the simulations including rolls. The destabilisation effect close to the end of the potential core associated with an increase of the phase velocity close to the nozzle observed for high roll amplitude may act to counterbalance the acoustically beneficial trends observed for SPOD-streaks.

Non-trivial changes in the wavepacket shape are observed for resolvent-streaks of higher amplitude, which can be induced by the strong dips in the ξ plot in figures 6(a,b). To illustrate that, the shapes of the equivalent axisymmetric mode (obtained by azimuthally averaging the resulting modes from PSE) are shown in figures 8 ($A_s = 6\%$) and 9 ($A_s = 16\%$) for SPOD-streaks (a), resolvent-streaks (b), and resolvent-streaks and rolls (c). For low amplitude streaks without rolls (figure 8(a,b)), the shapes of the KH mode are qualitatively similar to a non-modulated wavepacket (see, for instance Lesshafft *et al.* (2019)), and the stabilisation can only be perceived in comparison with the axisymmetric PSE. If rolls are included, two features become apparent: first, the wavepacket peak shifts slightly upstream, which is in line with the stabilisation trend observed in figure 6(b); at the same time, tilted structures are amplified across the shear layer, which are observed mostly downstream. For the highest streak amplitude (figure 9), the same tilted structure is observed, suggesting that the shapes of the resolvent-streaks and the presence of the rolls triggers the development of these structures for lower A_s. In figure 9(b,c),

it is shown that high amplitude resolvent-streaks strongly amplify the growth of these structures, which become dominant over the axisymmetric wavepacket. The appearance of these tilted modes may be associated with the mode-shifting phenomenon observed in the locally parallel framework (Lajús *et al.*, 2019), which may lead to a change in the mode being marched by the PSE. They may also be correlated to the appearance of oblique waves by the presence of a streaky base flow, as shown in Nogueira & Cavalieri (2021). The effect of these structures in the acoustic field is still unknown, and such evaluation will be left as a future endeavour.

Conclusions

A PSE formulation is used to evaluate the changes in the wavepacket hydrodynamic characteristics induced by the presence of streaks. The latter are obtained either from SPOD applied to PIV data, or from resolvent analysis, which allows us to consider the influence of rolls in the development of the KH mode. It is shown that, for SPOD-streaks (which are more radially spread across the shear layer), these structures have a stabilising effect on the KH mode; increasing streak amplitude A_s and azimuthal wavenumber m_s further enhances that trend, which may lead to a mitigation of the sound generated by the axisymmetric wavepacket. It is also shown that the phase velocity of the resulting mode is slightly reduced further downstream due to the presence of these elongated structures. A similar trend is observed for resolvent-streaks of low/moderate amplitudes. However, since these structures are more radially compact, their presence induces stronger local shear, which further enhances the signature of tilted structures in the velocity field. The overall effect of these streaks involves the development of regions of stabilisation and destabilisation depending on A_s.

It is important to highlight that, even though the present formulation may be able to provide a first approximation of the effect of streaks and rolls in the wavepacket characteristics, it also has some limitations. The first is that this formulation only considers a one-way coupling between streaks and wavepackets, which means that streaks affect the KH mode, but the development of the KH does not affect the streaks. This assumption of "frozen" mean flow may be too stringent, as suggested by Nogueira & Cavalieri (2021), and can only capture part of the dynamics. Secondly, it is well known that PSE struggles to capture non-modal behaviour (Towne *et al.*, 2019). Considering that high azimuthal wavenumber KH modes are active closer to the nozzle, and the mode-shift observed downstream, it is possible that PSE fails to closely capture the phenomenon at higher x/D. A possible workaround is to solve the One-Way Navier Stokes equations for the same problem, which mitigates the limitations of PSE. This will be performed in the next steps of this project, which will also include a comprehensive experimental campaign to confirm the trends observed herein.

REFERENCES

Alkislar, M. B., Krothapalli, A. & Butler, G. W. 2007 The effect of streamwise vortices on the aeroacoustics of a mach 0.9 jet. *Journal of Fluid Mechanics* **578**, 139–169.

Cavalieri, A. V. G., Jordan, P., Colonius, T. & Gervais, Y. 2012 Axisymmetric superdirectivity in subsonic jets. *Journal of Fluid Mechanics* **704**, 388.

Cavalieri, A. V. G., Jordan, P. & Lesshafft, L. 2019 Wave-Packet Models for Jet Dynamics and Sound Radiation. *Applied Mechanics Reviews* **71** (2), 020802.

Cavalieri, A. V. G., Rodríguez, D., Jordan, P., Colonius, T. & Gervais, Y. 2013 Wavepackets in the velocity field of turbulent jets. *Journal of Fluid Mechanics* **730**, 559–592.

Edgington-Mitchell, D., Honnery, D. R. & Soria, J. 2015 Staging behaviour in screeching elliptical jets. *International Journal of Aeroacoustics* **14** (7), 1005–1024.

Ellingsen, T. & Palm, E. 1975 Stability of linear flow. *The Physics of Fluids* **18** (4), 487–488.

Gudmundsson, K. & Colonius, T. 2011 Instability wave models for the near-field fluctuations of turbulent jets. *Journal of Fluid Mechanics* **689**, 97–128.

Herbert, T. 1994 Parabolized stability equations. *Special Course on Progress in Transition Modelling (AGARD)* **793**, 1–34.

Herbert, T. 1997 Parabolized stability equations. *Annual Review of Fluid Mechanics* **29** (1), 245–283.

Jordan, P. & Colonius, T. 2013 Wave packets and turbulent jet noise. *Annual Review of Fluid Mechanics* **45** (1).

Lajús, F. C., Sinha, A., Cavalieri, A. V. G., Deschamps, C. J. & Colonius, T. 2019 Spatial stability analysis of subsonic corrugated jets. *Journal of Fluid Mechanics* **876**, 766–791.

Lesshafft, L., Semeraro, O., Jaunet, V., Cavalieri, A. V. G. & Jordan, P. 2019 Resolvent-based modeling of coherent wave packets in a turbulent jet. *Phys. Rev. Fluids* **4**, 063901.

Nogueira, P. A. S. & Cavalieri, A. V. G. 2021 Dynamics of shear-layer coherent structures in a forced wall-bounded flow. *Journal of Fluid Mechanics* **907**, A32.

Nogueira, P. A. S., Cavalieri, A. V. G., Jordan, P. & Jaunet, V. 2019*a* Large-scale streaky structures in turbulent jets. *Journal of Fluid Mechanics* **873**, 211–237.

Nogueira, P.A. S., Cavalieri, A. V. G., Schmidt, O. T., Jordan, P., Jaunet, V., Pickering, E., Rigas, G. & Colonius, T. 2019*b* Resolvent-based analysis of streaks in turbulent jets. In *25th AIAA/CEAS Aeroacoustics Conference*, p. 2569.

Pickering, E., Rigas, G., Nogueira, P. A. S., Cavalieri, A. V. G., Schmidt, O. T. & Colonius, T. 2020 Lift-up, Kelvin–Helmholtz and Orr mechanisms in turbulent jets. *Journal of Fluid Mechanics* **896**, A2.

Pickering, E., Rigas, G., Schmidt, O. T., Sipp, D. & Colonius, T. 2021 Optimal eddy viscosity for resolvent-based models of coherent structures in turbulent jets. *Journal of Fluid Mechanics* **917**, A29.

Schmidt, O. T., Towne, A., Rigas, G., Colonius, T. & Brès, G. A. 2018 Spectral analysis of jet turbulence. *Journal of Fluid Mechanics* **855**, 953–982.

Sinha, A., Gudmundsson, K., Xia, H. & Colonius, T. 2016 Parabolized stability analysis of jets from serrated nozzles. *Journal of Fluid Mechanics* **789**, 36–63.

Tissot, G., Lajús Jr, F. C., Cavalieri, A. V. G. & Jordan, P. 2017 Wave packets and orr mechanism in turbulent jets. *Physical Review Fluids* **2** (9), 093901.

Towne, A., Rigas, G. & Colonius, T. 2019 A critical assessment of the parabolized stability equations. *Theoretical and Computational Fluid Dynamics* **33** (3), 359–382.

Towne, A., Schmidt, O. T. & Colonius, T. 2018 Spectral proper orthogonal decomposition and its relationship to dynamic mode decomposition and resolvent analysis. *Journal of Fluid Mechanics* **847**, 821–867.

Violato, D. & Scarano, F. 2011 Three-dimensional evolution of flow structures in transitional circular and chevron jets. *Physics of Fluids* **23** (12), 124104–124104.

Wang, C., Lesshafft, L., Cavalieri, A. V. G. & Jordan, P. 2021 The effect of streaks on the instability of jets. *Journal of Fluid Mechanics* **910**.

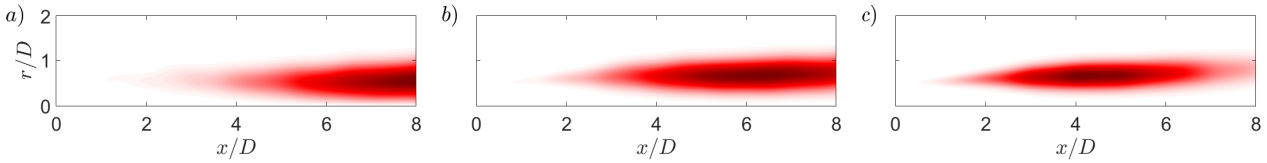

Figure 1. Absolute value of streamwise velocity fluctuations obtained from SPOD data for $m_s = 2$ (a), 4 (b) and 6 (c).

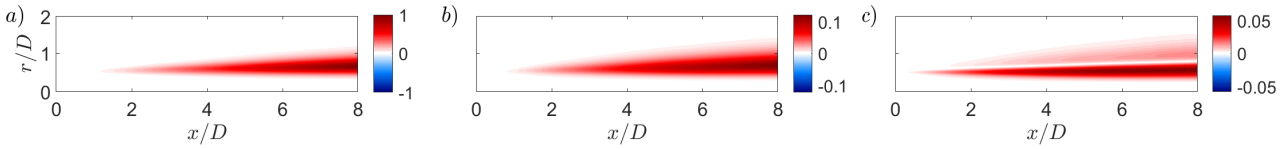

Figure 2. Absolute value of streamwise (a), radial (b) and azimuthal (c) velocity fluctuations from resolvent analysis for $m_s = 6$.

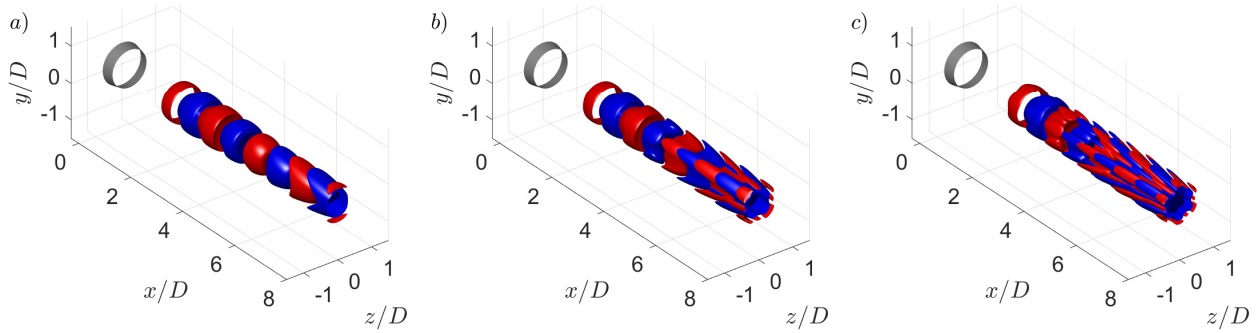

Figure 3. Isocontours of 30% of the maximum streamwise velocity from PSE (real part) for $St = 0.4$ and $m_s = 2$ (a), 4 (b) and 6 (c). Streaks obtained from SPOD with amplitude chosen as $A_s = 6\%$.

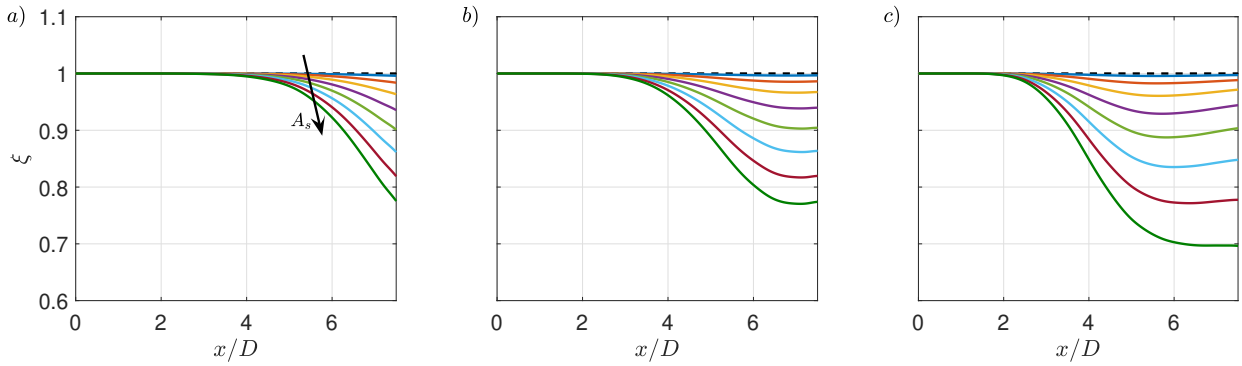

Figure 4. Attenuation of the KH mode at the centreline for increasing streak amplitude. Streaks obtained from SPOD with amplitudes varying in the interval $A_s = [0, 16\%]$ for $m_s = 2$ (a), 4 (b) and 6 (c) and $St = 0.4$. Dashed lines indicate the $A_s = 0$ case.

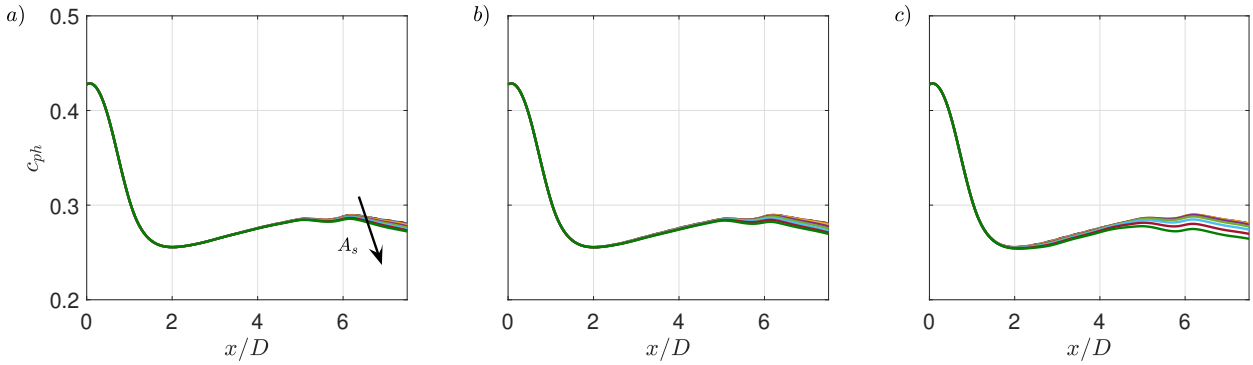

Figure 5. Phase velocity of the KH mode as function of the streamwise coordinate for increasing streak amplitude. Streaks obtained from SPOD with amplitudes varying in the interval $A_s = [0, 16\%]$ for $m_s = 2$ (a), 4 (b) and 6 (c) and $St = 0.4$. Dashed lines indicate the $A_s = 0$ case.

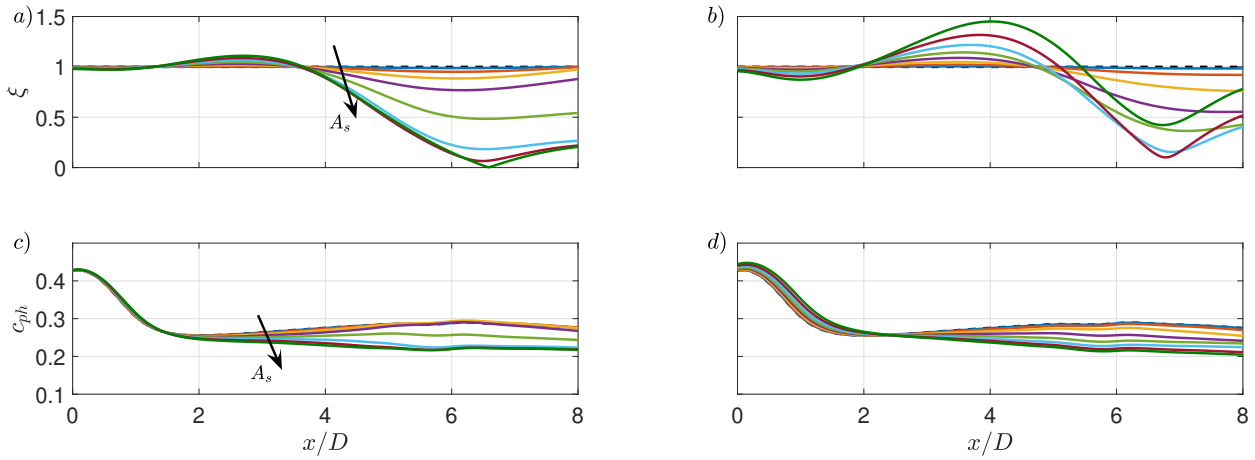

Figure 6. Attenuation (a,b) and phase velocity (c,d) of the KH mode as function of the streamwise coordinate for increasing streak amplitude without (a,c) and with (b,d) rolls. Streaks and rolls obtained from resolvent analysis with amplitudes varying in the interval $A_s = [0, 16\%]$ for $m_s = 6$ and $St = 0.4$. Dashed lines indicate the $A_s = 0$ case.

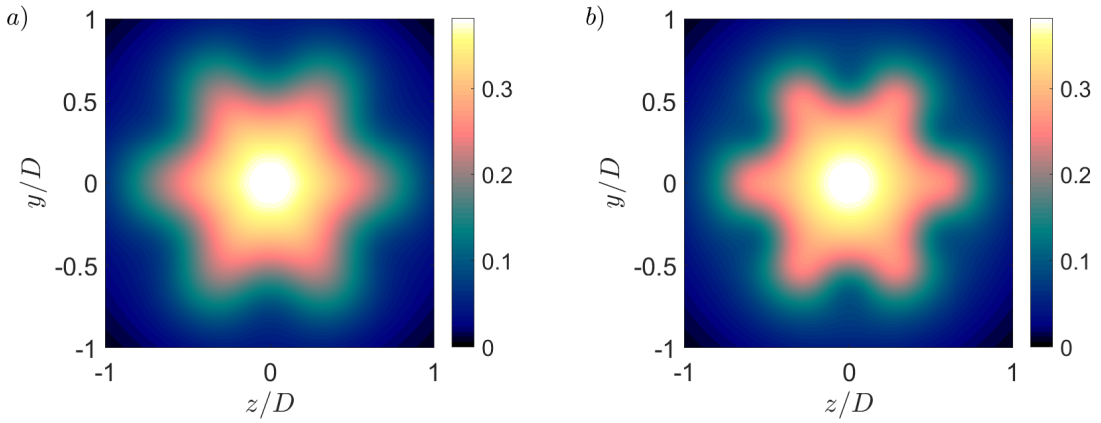

Figure 7. Mean streamwise velocity build using SPOD (a) and resolvent (b) streaks at $x/D = 6$, $m_s = 6$ and $A_s = 16\%$.

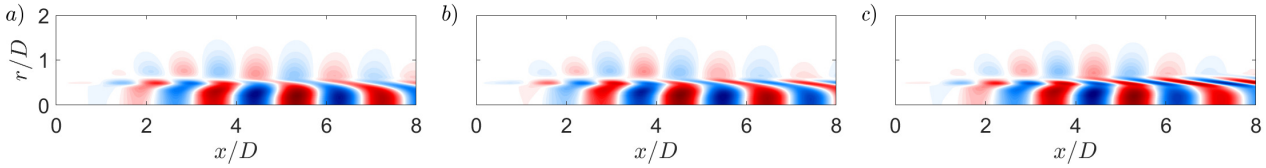

Figure 8. Real part of streamwise velocity fluctuations obtained from PSE for $St = 0.4$, $m_s = 6$ and $A_s = 6\%$. Streaks obtained from SPOD (a) and resolvent without (b) and with (c) rolls.

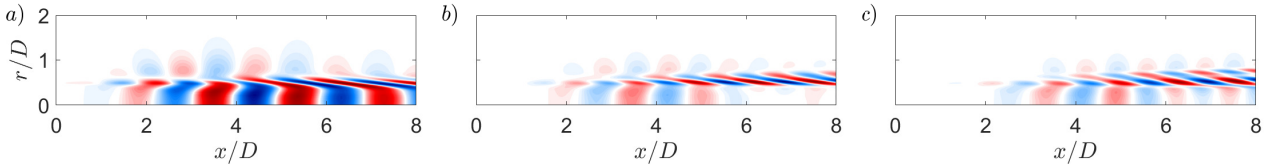

Figure 9. Real part of streamwise velocity fluctuations obtained from PSE for $St = 0.4$, $m_s = 6$ and $A_s = 16\%$. Streaks obtained from SPOD (a) and resolvent without (b) and with (c) rolls.